SPAWAR
Systems Center
PACIFIC

Technical Report 3032
December 2016

San Clemente Island Baseline LiDAR Mapping
Final Report

D. Bart Chadwick, Ph.D.
Jennifer Ayers, Ph.D.
William Wild
SSC Pacific

Adam Young, Ph.D.
Ken Melville, Ph.D.
Nick Statom
Luc Lenain
Reinhard Flick, Ph.D.
SIO UCSD

SSC Pacific
San Diego, CA 92152-5001

SSC Pacific
San Diego, California 92152-5001

K. J. Rothenhaus, CAPT, USN
Commanding Officer

C. A. Keeney
Executive Director

ADMINISTRATIVE INFORMATION

The work described in this report was performed for Commander, U.S. Pacific Fleet, Pearl Harbor, HI, by the Environmental Sciences Branch (Code 71750) and the Energy & Environmental Sustainability Branch (Code 71760), Space and Naval Warfare Systems Center Pacific, San Diego, CA.

Released by
R. George, Head
Energy & Environmental Sustainability Branch

Under authority of
A. J. Ramirez, Head
Advanced Systems & Applied Sciences Division

SB

EXECUTIVE SUMMARY

U.S. Pacific Fleet (PACFLT) requires high-resolution topographic data of San Clemente Island (SCI) to support management of the island's natural resources. Such a dataset will enable tracking of changes in erosion patterns, which may be precursors to training impacts on species and their habitats. In response to this need, this work effort generated several high-resolution, georeferenced aerial remote sensing data sets of SCI. This report describes the data deliverables and the analysis that has been done with them.

Data collection flights were flown in September and October 2014. Deliverables include high-resolution Light Detection and Ranging (LiDAR) point data (10-cm vertical accuracy); georeferenced first and last return digital elevation models (DEMs) on a 1 m x 1 m grid, high-resolution hyperspectral data cubes (126 bands with ~5-nm spectral resolution), and georeferenced aerial photographs. Ground truth data collected by Space and Naval Warfare Systems Center Pacific (SSC Pacific) and PACFLT during September to November 2014 is also included with the data distribution.

The data deliverables are a baseline data set that can be used as a point of comparison for future high-resolution monitoring, as well as historical topographic change detection. Existing 2002 and 2013 digital elevation models (DEMs) of the island were used for topographic change detection. Erosion and accretion with volumes >2.5 m^3 were successfully detected from 2013 to 2014. The changes appear mostly related to changes to dirt roads, parking lots, and construction. Though the relatively poor elevation accuracy of the historical DEMs limited change detection capability, they show proof of concept for SCI. We estimate that with a future LiDAR data set of comparable quality to the current deliverable (2014 data), changes with volumes as small as 1 m^3 will be detectable.

Erosion analysis was also conducted using just the 2014 DEM deliverable. Most erosion is gullying due to water. Erosion due to munitions impacts is seen in target range areas on the southwest corner of the island. Here hundreds of craters, typically 3-50 m^2 and several meters deep, are detectable. These will likely have altered the natural drainage patterns.

Finally, the high-resolution data deliverables generated from this work open up almost limitless possibilities for future data analysis. We briefly explore some of these. Rugosity metrics derived from the LiDAR data appear to have promise for automatically identifying structures such as vegetation and buildings. Using the aerial photographs in conjunction with the ground truth data, we could automatically detect individual shrubs, though this method was more successful in some places than others. Finally, the hyperspectral data cubes, with both high spatial and spectral resolution, may be leveraged to answer many detailed questions about land cover. The addition of coincident ground truth spectra further enhances the capability of this powerful data set.

To best support monitoring and management of the natural resources on San Clemente Island, return flights roughly every two years would be beneficial.

ACRONYMS AND ABBREVIATIONS

BIL	band-interleaved-by-line, a type of binary format
.dat	radiance data file
DEM	Digital Elevation Model
ENVI	“Environment for Visualizing Images”, a software package for hyperspectral imagery analysis
GLT	ENVI “Geographic Lookup Table” file
IDL	“Interactive Data Language”, a programming language that can access ENVI algorithms
ifSAR	Interferometric Synthetic Aperture Radar
IGM	Input Geometry data file
.kml	Google Earth File
.las	Laser Point File (.las) containing LiDAR point cloud data
LiDAR / Lidar	Light Detection and Ranging
mW	milliwatt
PACFLT	U.S. Pacific Fleet
RGB	Red, Green, and Blue bands of the electromagnetic spectrum
RMS	Root Mean Square, a measure of error
SCI	San Clemente Island
SLR	Single Lens Reflex, referring to a camera or its images
SIO	Scripps Institution of Oceanography
sr	steradian
SSC Pacific	Space and Naval Warfare Systems Center Pacific
TPI	Topographic Position Index
µm	micrometer
UTM	Universal Transverse Mercator coordinate system

CONTENTS

Figures

Tables

1. INTRODUCTION

Commander, U.S. Pacific Fleet (USPACFLT) requires high-resolution topographic data of San Clemente Island (SCI) to support management of the island's natural resources in a manner that promotes the sustainable use of training areas. SCI is the primary maritime training area for the Department of the Navy, Pacific Fleet, and the U.S. Navy SEALS, and also supports training by the U.S. Marine Corps, U.S. Air Force, and other users. As the southernmost of California's Channel Islands, San Clemente is also home to a variety of rare terrestrial and marine resources, including 24 listed as endangered or threatened under the Endangered Species Act. More than a century of overgrazing and browsing by non-native herbivores dramatically reduced vegetation cover on the island, accelerating soil erosion. Although native vegetation has been recovering across much of the island following the removal of the last feral herbivore in the early 1990s, sustainable use of the island for its military mission and the continued recovery of sensitive natural resources require monitoring and management of soil erosion. High resolution topographic data are needed to track erosion rates and patterns, which will allow corrective management measures to be implemented before erosion results in adverse impacts to sensitive species or their habitats. While high-resolution topographic data have been collected along the majority of the California coast via Light Detection and Ranging (LiDAR or lidar), prior to this work no such data existed for San Clemente Island.

In response to this need, this work effort generated a georeferenced, high-resolution LiDAR data set of SCI. Supplemental hyperspectral data cubes and visible single-lens reflex (SLR) photographs were also collected. This accurate georeferenced baseline data set can be used as a point of comparison for future high-resolution monitoring. Subsequent overflights will enable small-scale change detection related to natural and anthropogenic erosion and accretion, as well as vegetation change. The data can also be used for comparison with existing historical low-to-medium resolution data of the island.

This report describes the data collection, processing, and data deliverables (LiDAR, hyperspectral, and SLR photographs). It also provides analysis of the LiDAR data, including data accuracy, historical topographical change detection, a description and characterization of SCI erosional features, and a discussion of the potential of LiDAR data for vegetation characterization.

2. DATA DELIVERABLES

2.1 DATA COLLECTION

Data were collected on September 23–25 2014, and October 7–8, 2014, by Scripps Institution of Oceanography (SIO) using its Modular Aerial Sensing System (MASS). Instruments on the MASS include a full-waveform LiDAR (Riegl® Q680i), a hyperspectral sensor (Specim AISA EAGLE), an SLR camera, and supporting instruments for geolocation and orthorectification (Figure 1). Data deliverables are listed in Section 2.2 and described in Section 2.3.

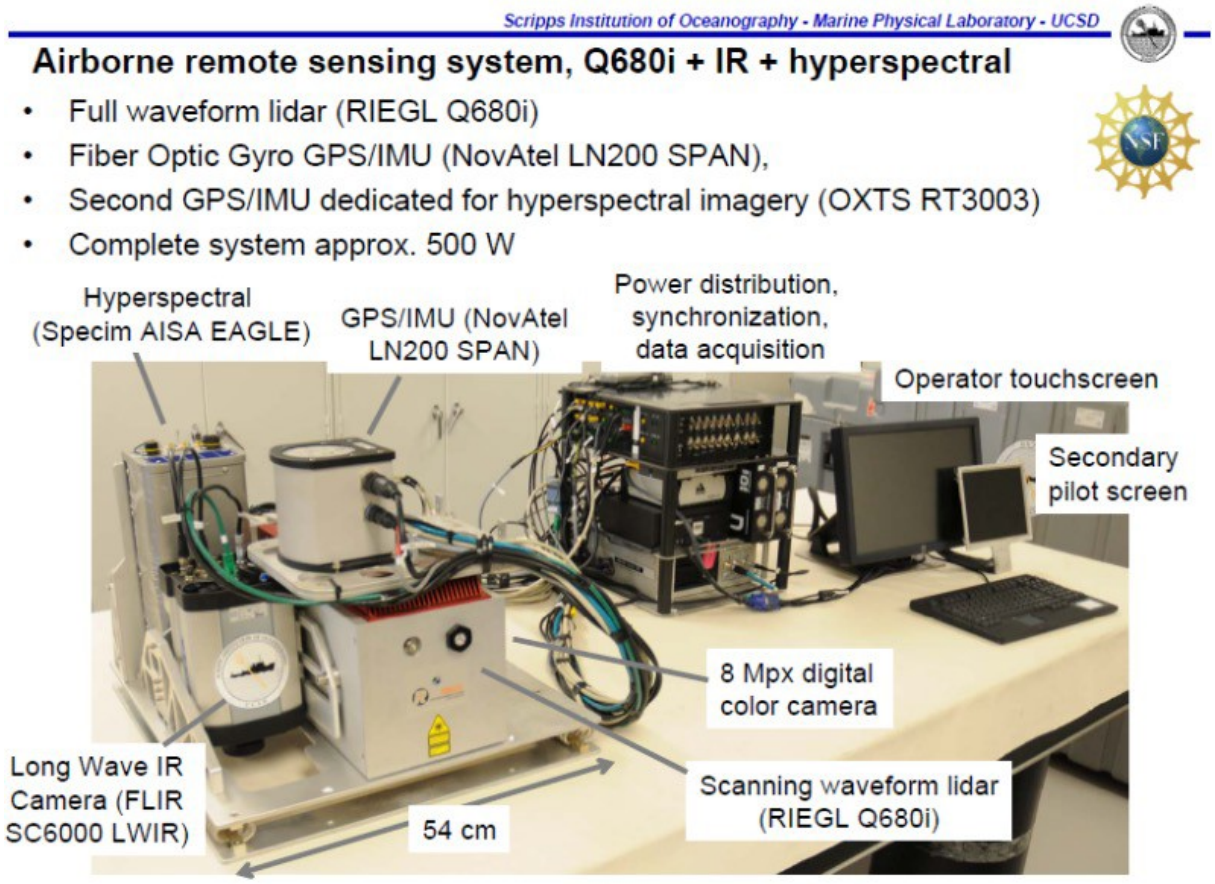

Figure 1. The Scripps Institution of Oceanography Modular Aerial Sensing System (MASS) used for data collection.

2.2 FILE STRUCTURE

All remote sensing data are delivered on two external hard drives. Processing Level 1 is the lowest level and Processing Level 3 is the highest. Most users will prefer to use data that are at higher processing levels. The file structure is as follows:

SanClemente_Disk1

- 1.0 LiDAR
  - 1.1 DEM
    - SCI_FirstReturn.tif
    - SCI_FirstReturn.tfw
    - SCI_LastReturn.tif
    - SCI_LastReturn.tfw
  - 1.2 LASPointCloud
    - SCI_Color_Point_Cloud_Data_20140923
      - 20140923_SCI_3629285N_0367179E.las
      - and many more .las files
    - SCI_Color_Point_Cloud_Data_20140924
    - SCI_Color_Point_Cloud_Data_20140925
    - SCI_Color_Point_Cloud_Data_20141007
    - SCI_Color_Point_Cloud_Data_20141008
  - 1.3 Point Statistics Rasters
    - Density.tif
    - Max.tif
    - Mean.tif
    - Min.tif
    - Range.tif
    - Stdev.tif
- 2.0 Hyperspectral
  - 2.1 ProcessingLevel_1
    - IGM
      - *scene*_radiance_IGM.txt
    - RAD
      - *scene*_radiance.dat
      - *scene*_radiance.hdr

2.2 ProcessingLevel_2

XY_tiffs

*scene*_X.tif
*scene*_Y.tif

RAD_clean

*scene*_radiance.dat
*scene*_radiance.hdr

ENVI_GLT

*scene*_GLT
*scene*_GLT.HDR

2.3 ProcessingLevel_3

RAD_rgb_georeferenced

*scene*_georefd_rgb.dat
*scene*_georefd_rgb.hdr

RAD_allbands_georeferenced

09232136_georefd.dat
09232136_georefd.hdr

There are 75 hyperspectral *scenes*:

0923-2136	0924-2308	0925-2351	1007-2145	1007-2354
0923-2147	0924-2321	0926-0003	1007-2150	1008-0002
0923-2152	0924-2334	0926-0015	1007-2159	1008-0008
0923-2204	0925-2024	0926-0023	1007-2208	1008-2114
0923-2215	0925-2136	0926-0030	1007-2216	1008-2117
0923-2220	0925-2148	0926-0037	1007-2224	1008-2122
0923-2232	0925-2201	0926-0043	1007-2233	1008-2127
0923-2249	0925-2213	0926-0050	1007-2240	1008-2131
0924-2101	0925-2226	0926-0057	1007-2248	1008-2138
0924-2147	0925-2238	0926-0100	1007-2256	1008-2141
0924-2155	0925-2250	0926-0102	1007-2303	1008-2149
0924-2206	0925-2303	1007-2031	1007-2310	1008-2206
0924-2218	0925-2315	1007-2129	1007-2315	1008-2225
0924-2244	0925-2327	1007-2134	1007-2325	1008-2233
0924-2255	0925-2339	1007-2139	1007-2342	1008-2235

For each scene, there is one of each file type in the file structure shown above.

3.0 Ground Truth

3.1 GPS_data

Excel

bare_low_sep.xlsx
bare_nov.xlsx
low_nov.xlsx
rock_nov.xlsx
shrub_nov.xlsx
shrub_oct.xlsx
shrub_sep.xlsx

GIS

Same files as Excel, but as ArcGIS® shape files

Text

Same files as Excel, but as plain text

3.2 Photographs

665 photographs, in folders by date

3.3 Spectra

827 spectra, matching GPS_data

SanClemente_Disk2

1.0 SLR Photographs

1.1 ProcessingLevel_1, not generated

20140923

JPEG_RAW [folder of raw jpegs]
TIFF_8BIT [folder of raw tiffs]
SCI_20140923_DSLR_Metadata.csv
SCI_20140923_KML_MSL.kml

20140924 [contents same as above]
20140925 [contents same as above. Photos from 0926 are also in this folder]
20141007 [contents same as above]
20141008 [contents same as above]

1.2 ProcessingLevel_2, orthorectified and georeferenced [geotiffs]

4,536 files (1,452 scenes)

2.3 DESCRIPTION OF FILES

2.3.1 LiDAR

2.3.1.1 DEMs (Digital Elevation Models)

The DEMs are geotiffs, which are tiffs that contain location data. They consist of .tif and associated .tfw (tiff world) files, and can be opened like regular tiffs. Good options for viewing these include ArcGIS and ENVI.

There are two different DEMS included:

1. SCI_FirstReturn is a digital elevation model of the first return of the LiDAR. Theoretically, this is the height of the vegetation canopy. In practice it does not work very well for California coastal shrub land, likely because the LiDAR tends not to penetrate the dense shrub, resulting in nearly identical first and last return digital elevation models.
2. SCI_LastReturn is a digital elevation model of the last return of the LiDAR, considered a bare earth model.

2.3.1.1 LiDAR Point Cloud Files

LiDAR point cloud (.las) files contain the return data from the laser, and can be viewed with a variety of commercial software, including this freeware: Applied Imagery Quick Terrain Reader (http://appliedimagery.com/download/). The DEMs were made from processed point cloud data.

2.3.1.2 Point Statistics Rasters

Statistics on the LiDAR point returns are included in the data distribution as rasters (tiffs): point density; and maximum, minimum, mean, and standard deviation of point elevation. They were calculated on the same 1 m x 1 m grid as the DEM.

2.3.2 Hyperspectral Data

There are 75 overlapping hyperspectral scenes covering San Clemente Island. Each of these scenes is delivered at three levels of processing.

2.3.2.1 Processing Level 1

Level 1 data are the least processed (though not raw) data, and are not georeferenced, though they come with associated location information in a text file. Each Level 1 scene has a .dat, .hdr, and input geometry (IGM) file, as described below. Level 1 data are included in the data distribution for completeness, but it is anticipated most users will only use Level 2 and Level 3 data.

- RAD folder
  - *scene*_radiance.dat

  These files are radiometrically corrected images in binary BIL (band-interleaved-by-line) format. Units for radiometric values are 1000 * mW/cm^2 * sr * µm. The data dimensions of each image are width x length x number of spectral bands. All images are 969 pixels wide. The length of each image is determined by the acquisition rate times the acquisition time for each flight line. All lines were captured at 80 Hz, but the acquisition time

depended upon the geometry of the island, so the length of the images varies. There are 126 spectral bands at approximately 5-nm resolution, covering ~600 nm of spectral range.

- *scene*_radiance.hdr

These files associate with each .dat file. The header files are ASCII text files, viewable with any text editor. They contain metadata describing the .dat files, including information such as image width, length, number of spectral bands, wavelength and spectral width of each band, and Global Positioning System (GPS) start/stop times.

- IGM folder
  - *scene*_radiance_IGM.txt

  IGM (Input Geometry) data files are ASCII text files that provide a UTM (Universal Transverse Mercator) coordinate for each pixel in the image. The San Clemente Island images are all in UTM zone 11. Easting and Northing (x and y) values are in meters.

2.3.2.2 Processing Level 2

We anticipate the majority of users will work mostly with Level 2 data. These are the full hyperspectral data cubes (126 bands) that are not georeferenced to keep file size down, but plug-and-play ready to be georeferenced in ENVI or ENVI+IDL.

The full (126 band) hyperspectral data cubes are not included as georeferenced files in the data distribution because of their overly large file size. One such georeferenced data cube has been included as an example (found in ProcessingLevel_3 → RAD_allbands_georeferenced). This file is 179 GB, far too large for most computers to work with, and thus not useful.

ENVI recommends working with non-georeferenced (Level 2) files to develop a work flow, and then to georeference only needed bands. Georeferencing can be done directly via the ENVI graphical interface, or via the IDL procedure file we have included. If desired, the IDL file can be used to automate georeferencing of multiple files, once the user has chosen the desired bands.

- ENVI_GLT
  - *scene*_GLT

  These are ENVI “Geographic Lookup Table” files. They contain map location data for each pixel in the radiance.dat files, in UTM Zone 11N coordinates. ENVI can georeference .dat radiance images directly from these files. These GLT files were created from the X and Y tiffs (below).

- RAD_clean
  - *scene*_radiance.dat

  These are radiance files just as in Level 1 data, except they are cleaned to correspond to the GLT files. The ENVI function “Georeference from GLT” will take Level 2 GLT and radiance files as input, and generate georeferenced output. Do not use Level 1 radiance files for this function; in most cases, they are slightly different sizes and will throw in an error if used as such.

- XY_tiffs

  - *scene*_X.tif, scene_Y.tif

  These files are intermediate files unlikely to be needed, as the GLT files are provided as the best way to georeference the radiance files. The X and Y tiffs were generated from the IGM file (by cleaning it and then writing it in the tiff format), and contain the map coordinate data for each pixel in the Level 2 radiance files.

2.3.2.3 Processing Level 3

Level 3 data are georeferenced hyperspectral scenes.

- RAD_rgb_georefereced

  This folder contains a georeferenced data cube (RGB bands only) for all 75 scenes. They can be opened directly in ENVI. These files provide a visual picture of each San Clemente Island scene, while keeping workable file sizes.

- RAD_allbands_georeferenced

  This folder contains a georeferenced data cube (all 126 bands) for just one scene, 0923-2136. The georeferenced radiance .dat file is 179 GB, too large for most computers to handle. This scene is included as an example to illustrate why all scenes are not delivered as georeferenced whole data cubes.

2.3.3 Ground Truth

The ground truth data were collected by SSC Pacific and PACFLT in September, October, and November 2014. Each location surveyed on the island has a photograph, a spectrum or spectra, GPS coordinate, and attribute table that includes information such as vegetation height and species name.

- GPS_data

  - Excel

  This folder contains the ground truth data in Microsoft® Excel format.

  - GIS

  This folder contains the same ground truth data, only as ArcGIS® shapefiles with attribute tables.

  - Text

  This folder contains the same ground truth data as plain text

- Photographs

  665 photographs, associated with the GPS data

- Spectra

  827 spectra, associated with the GPS data

- README.doc

2.3.4 SLR Photographs

2.3.4.1 Processing Level 1

Level 1 photographs are photographs from the SLR camera that have not been georeferenced. Each photograph is supplied in both .jpeg and .tiff format. The .kml file is a Google™ Earth file that shows the location on the island where each image was taken by image file number. The .csv is a comma-delimited file, readable in Microsoft® Excel, containing metadata such as image file name, location, and aircraft orientation. These photographs have associated location information on the level of the photograph, but not the pixel.

2.3.4.2 Processing Level 2

Level 2 photographs are georeferenced, orthorectified tiffs (geotiffs). These images have location information associated with each pixel.

3. LIDAR DATA ANALYSIS

3.1 DATA QUALITY

The digital elevation model (DEM) developed from the LiDAR data has a spatial resolution of 1 m x 1 m. The vertical accuracy is 10 cm, and the horizontal accuracy is ~1 m. The precision of the instrument is 20 mm (vertical) and <10 cm (horizontal) at the flight altitude of ~3000 ft above mean sea level (1200–3000 ft above SCI ground level). Details on how the accuracy was calculated, as well as the procedure used for making the DEM, are detailed in this section.

3.1.1 Accuracy

LiDAR point return vertical accuracy was assessed by comparing last return DEM (bare earth model) elevations to 10 ground control points. Results of the comparison are show in Table 1. The elevation difference ranged from -0.21 to 0.04 m, with a mean elevation difference of -0.04 m. The vertical root mean square difference (RMSZ, Federal Geographic Data Committee, 1998), which is a measure of the vertical error, was 0.098 m. Before comparison, ground control points were converted from the WGS 84 coordinate system to UTM, NAD83, navd88, using vdatum v3.4.

Table 1. Comparison of LiDAR elevation data to ground control points. UTM-X and UTM-Y are UTM eastings and northings, Z-control is ground control elevation in meters, Z-DEM is the LiDAR-derived DEM elevation from this work, and Z-Difference is the difference between the two.

ID	UTM-X	UTM-Y	Z-Control	Z-DEM	Z-Difference
1	352240.0249	3654633.751	56.9473	57.047	0.0997
2	352010.4992	3654526.212	52.52665	02.457	-0.0696
3	352006.112	3654108.672	55.6758	55.658	-0.0178
4	354925.9019	3652654.819	51.2795	51.321	0.0415
5	356598.9779	3646291.432	255.9141	255.87	-0.0441
6	360779.6334	3642866.345	479.8968	479.9	0.0032
7	365357.2039	3638804.175	586.8227	586.807	-0.0157
8	370712.7984	3634036.631	297.2562	297.082	-0.1742
9	365523.1856	3634279.639	350.6039	350.58	-0.0239
10	363289.5969	3636588.04	464.4253	464.21	-0.2153

3.1.2 Digital Elevation Models

3.1.2.1 Process for Creating the DEMs

Digital elevation models (DEMs) were created by first separating LiDAR point data into first, last, and all returns. ASCII xyzi (easting, northing, elevation, intensity) files were then created as tiles, each covering an area of 250 m x 250 m plus a 5 m buffer. DEMs of the first and last return tiles were generated at a 1-m x 1-m resolution in UTM Zone 11N, navd88 coordinate system. Initial DEM tiles were produced with a natural neighbor interpolation and a 5-m spatial restriction to maintain data gaps where no point data exists. Grid cells of the DEMs were aligned with the center located at UTM integers, consistent with the prior 2013 Aechelon LiDAR DEM. Finally, tiles were merged into first and last return DEMs with full island coverage. Comparison of the overlap elevations between tiles were consistent, indicating tile edge effects were eliminated during processing.

3.1.2.2 Quality Control of the DEMs

Quality control of the initial DEMs showed coastal areas with erroneous data, possibly from coastal fog. The “fog” areas were removed by reprocessing the DEMs without returns of intensity values less than 25. This threshold was determined by trial and error. Data gaps in the fog areas were filled by applying a clustering algorithm to all return point data, which separated fog and land returns for each empty fog grid cell. DEM fog cell values were assigned the mean elevation of the land point cluster. A few remaining data gaps in the fog areas were filled with a natural neighbor interpolation. After the DEM fog correction, a small number of erroneous spikes and pits were identified and corrected by using a 3 m x 3 m filter to generate final DEM products (Figure 2).

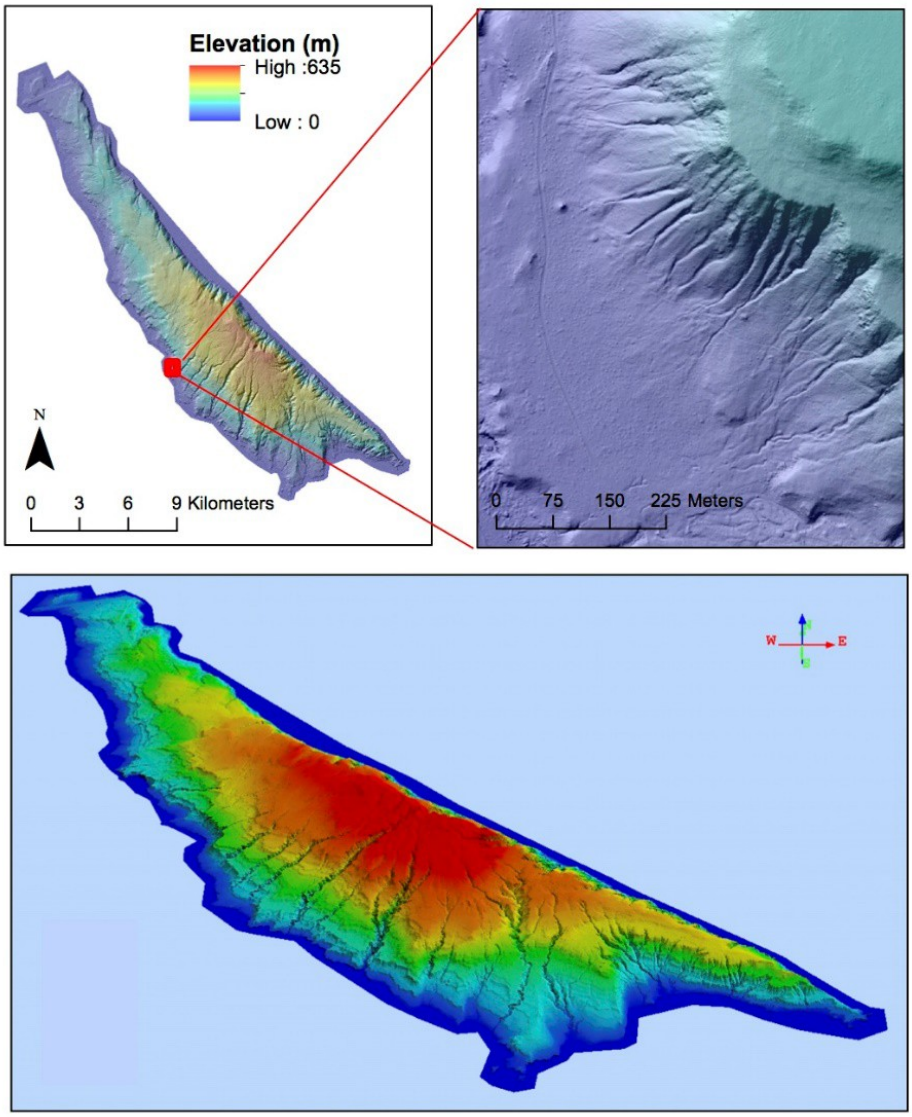

Figure 2. High resolution digital elevation map of San Clemente Island.

3.2 HISTORICAL TOPOGRAPHICAL CHANGE DETECTION

Topographic change for two time intervals was obtained by differencing historical DEMs, from 2002 and 2013, with the current 2014 DEM to create digital change grids. Both erosion (negative changes) and accretion (positive changes) were found. Sources of error in elevation change maps include the basic LiDAR observations, spatial interpolation, and vegetation.

3.2.1 Change Since 2002 ifSAR Survey

Topographical change since 2002 was analyzed using a DEM from an ifSAR survey. The DEM was downloaded from the National Oceanic and Atmospheric Administration (NOAA) coastal website (https://coast.noaa.gov/digitalcoast/) in gridded raster format, in the UTM coordinate system with navd88 vertical datum. The stated accuracy at the 95% confidence level is 4.3 m in the

horizontal dimension and 2.2 m in the vertical. The initial change map created showed systematic error between the 2002 DEM and the last return 2014 DEM (Figure 3). To correct for the bias, the 2002 DEM was shifted 5 m south, 5 m east, and 2.8 m down. These values were determined by trial and error and improved the alignment between the two digital elevation models (Figure 3). However, the adjusted change map shows numerous erroneous changes, and caution should be used when interpreting topographic changes between the 2002 to 2014 digital elevation models.

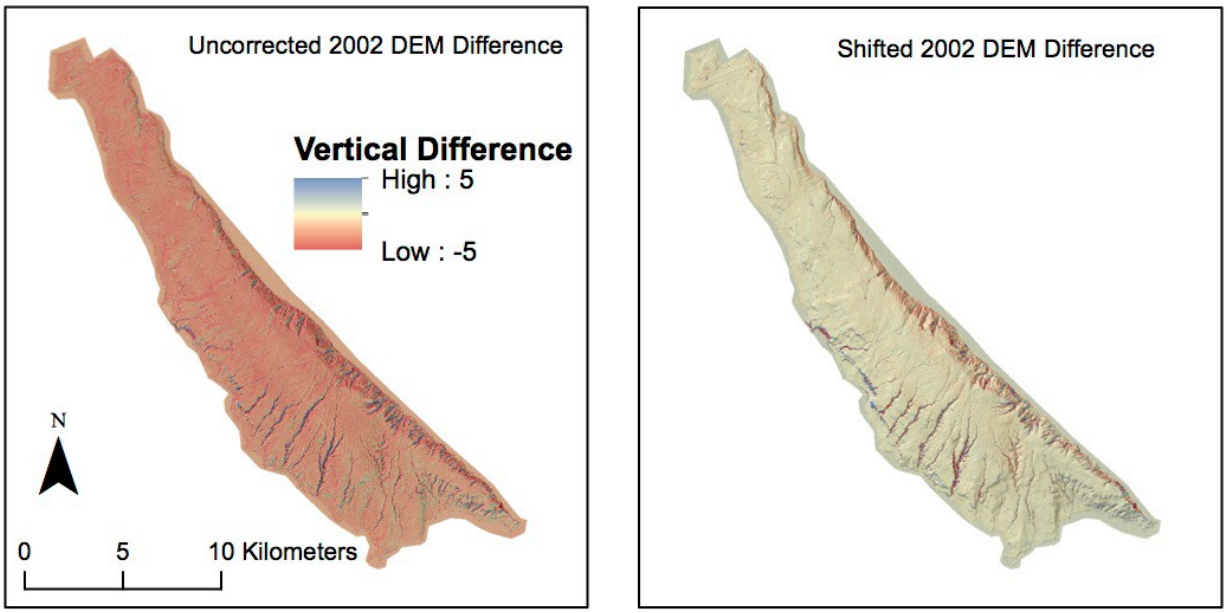

Figure 3. Left: Topographic change between the uncorrected 2002 and the 2014 DEM, showing systematic bias. Right: Adjusted 2002 and 2014 DEMs showing improved alignment.

The primary topographic changes between 2002 and 2014 that appear reliable were associated with dune movement on the northwest of the island. Figure 4 shows the dune front moving in a southeasterly direction at an average rate of about 1 to 2 m/yr.

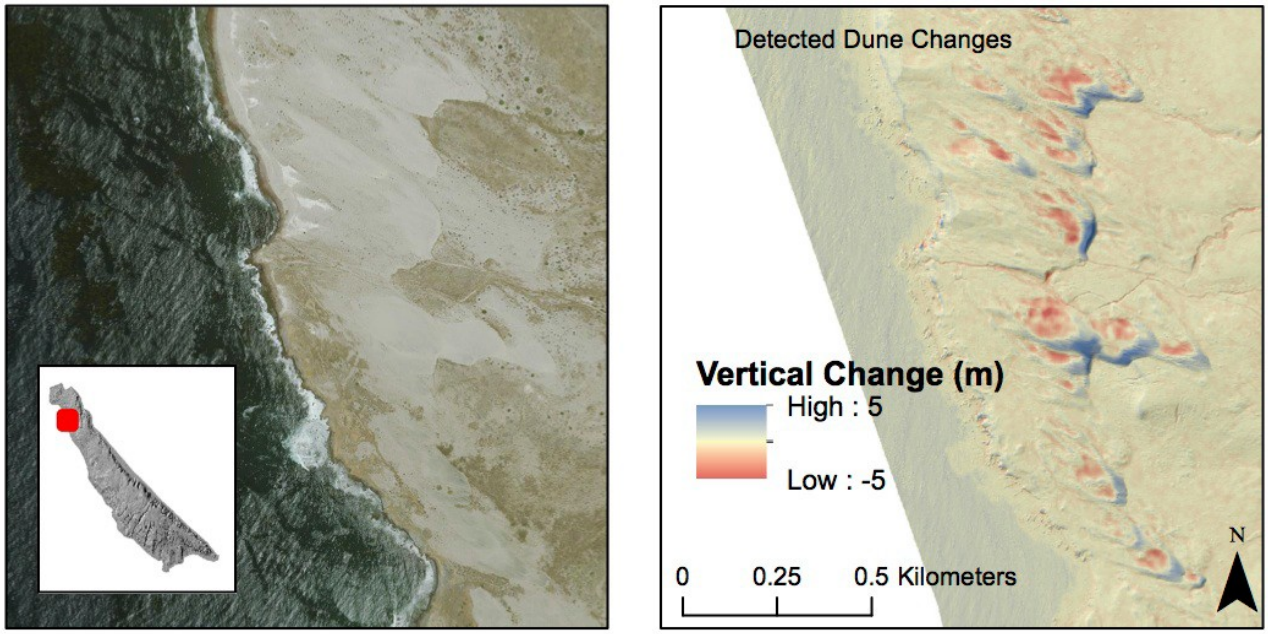

Figure 4. Detected topographic changes between 2002 and 2014 associated with dune processes.

3.2.2 Change Since 2013 Aechelon Survey

Topographic change since 2013 was analyzed using a DEM from an Aechelon survey. The vertical root mean square difference (RMSZ, Federal Geographic Data Committee, 1998), a measure of the total error, between the 2013 survey and the current 2014 DEM was estimated using the runway on the northern part of the island (area = 122,361m^2) as a control section assumed to experience no vertical change. The RMSZ for the 2013–2014 digital change grid was 11 cm. RMSZ increases for vegetated and sloped areas.

Change detection analysis was done in several steps. First, the digital change grids were filtered to remove noise and erroneous data. Next, all grid cells with a vertical change of less than 50 cm were neglected. 50 cm was chosen because it is much greater than the runway error of 11 cm, which is a low bound, as error increases in sloped and vegetated areas. This choice is conservative, designed to yield no false positive changes. Next, a minimum topographic footprint was imposed, requiring at least five connected cells of positive or negative change, thus enforcing a minimum change area of 5 m^2. This filtering identifies individual changes with a minimum volume of about 2.5 m^3 (if all 5 cells had 50 cm of change). Results of the filtering are shown in Figure 5. Filtering improves the reliability of the detected changes, but makes detection conservative because some actual changes are neglected. Vegetation, complex terrain, and slope make more detailed change detection in many areas difficult.

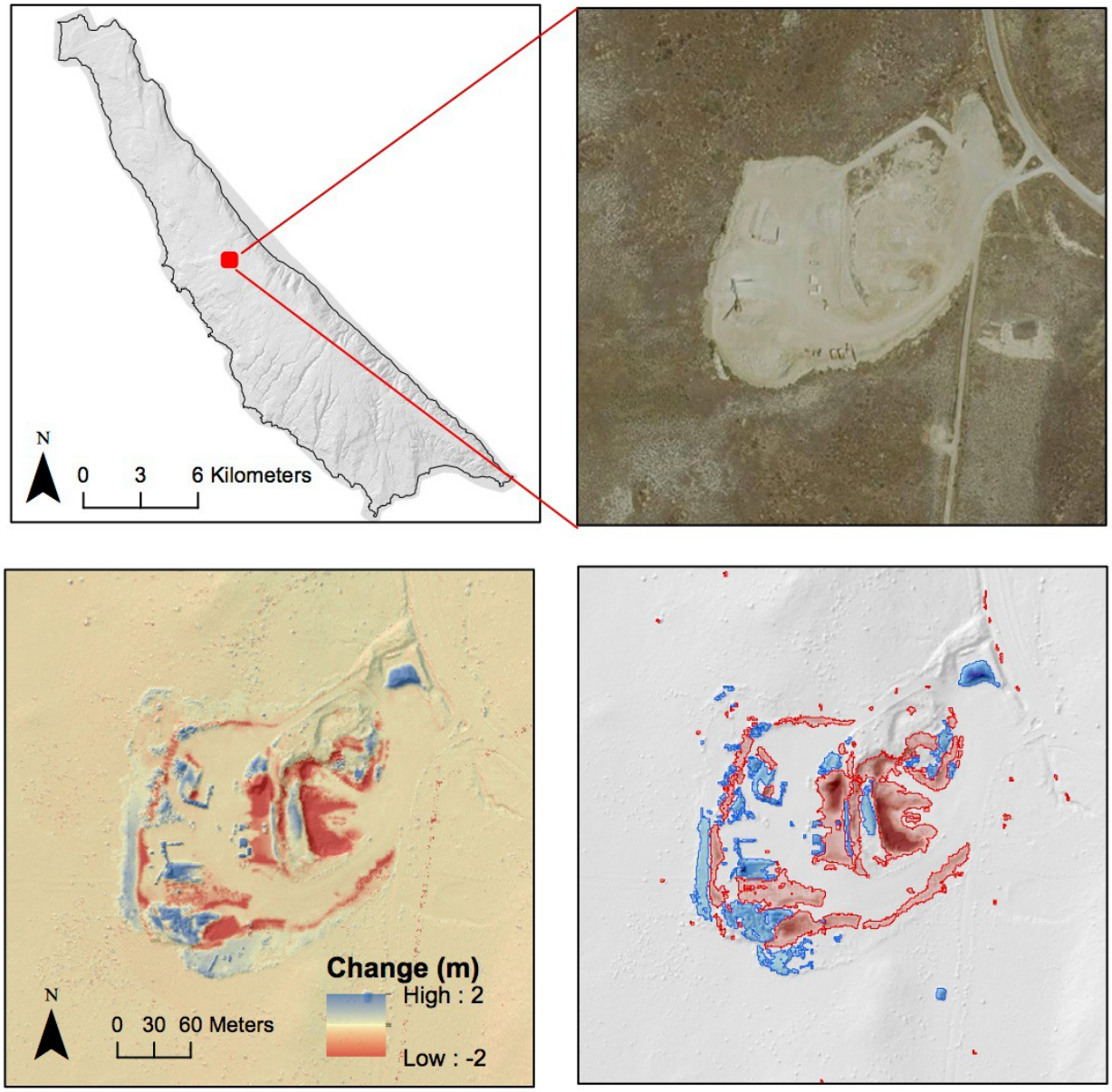

Figure 5. Example of detected topographic change from 2013–2014 (lower left), and those changes that meet filter thresholds to be extracted (lower right). The location is shown in the upper left, and an aerial photograph in the upper right. This is the site of an actively managed quarry.

The change detection analysis revealed minimal change in the course of one year's time. However, a few areas did experience elevation change, all apparently related to anthropogenic activity. These changes are shown in Figures 6–8.

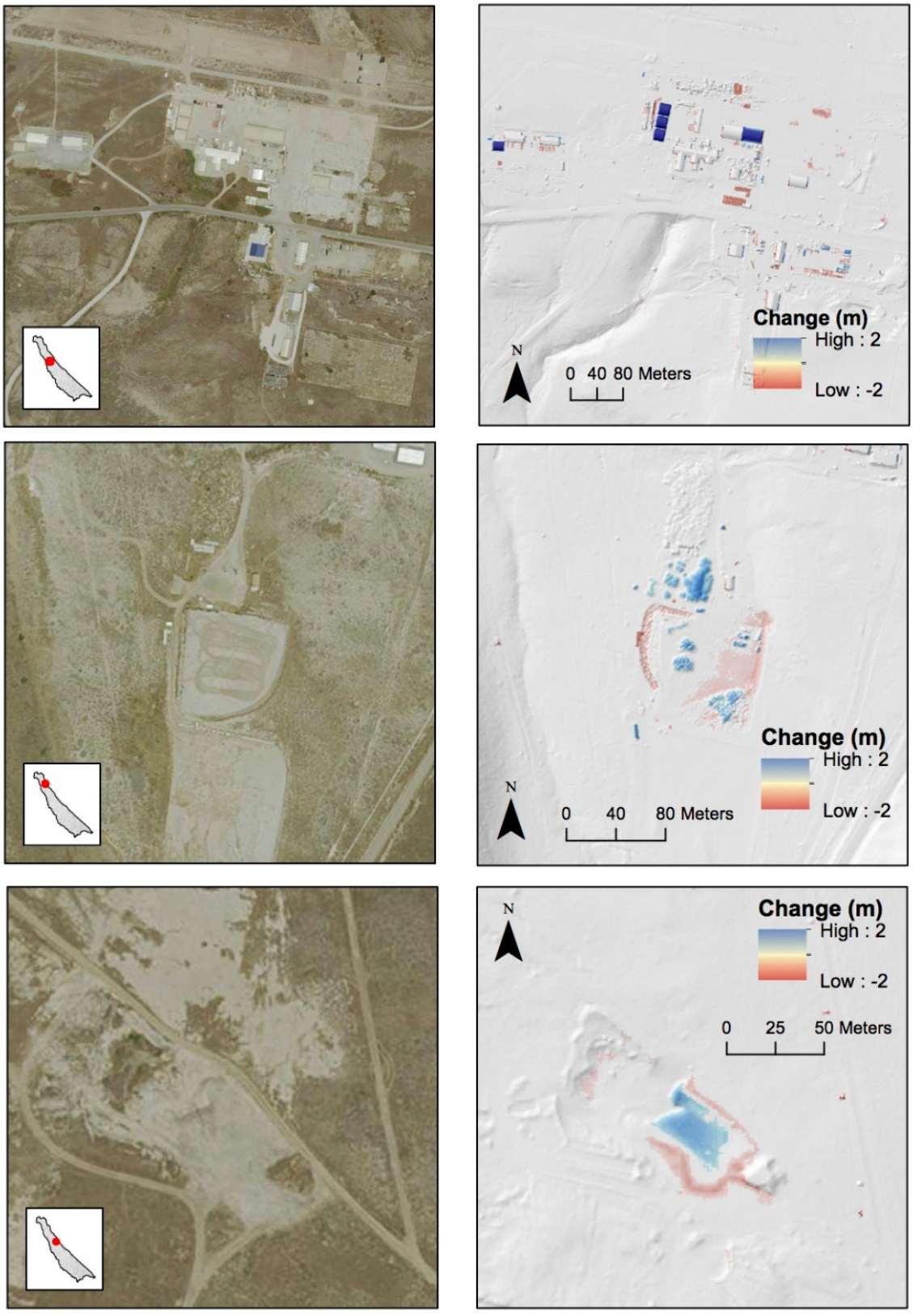

Figure 6. More areas of detected vertical change, 2013–2014 (right) and spatially corresponding 2014 aerial photographs (left).

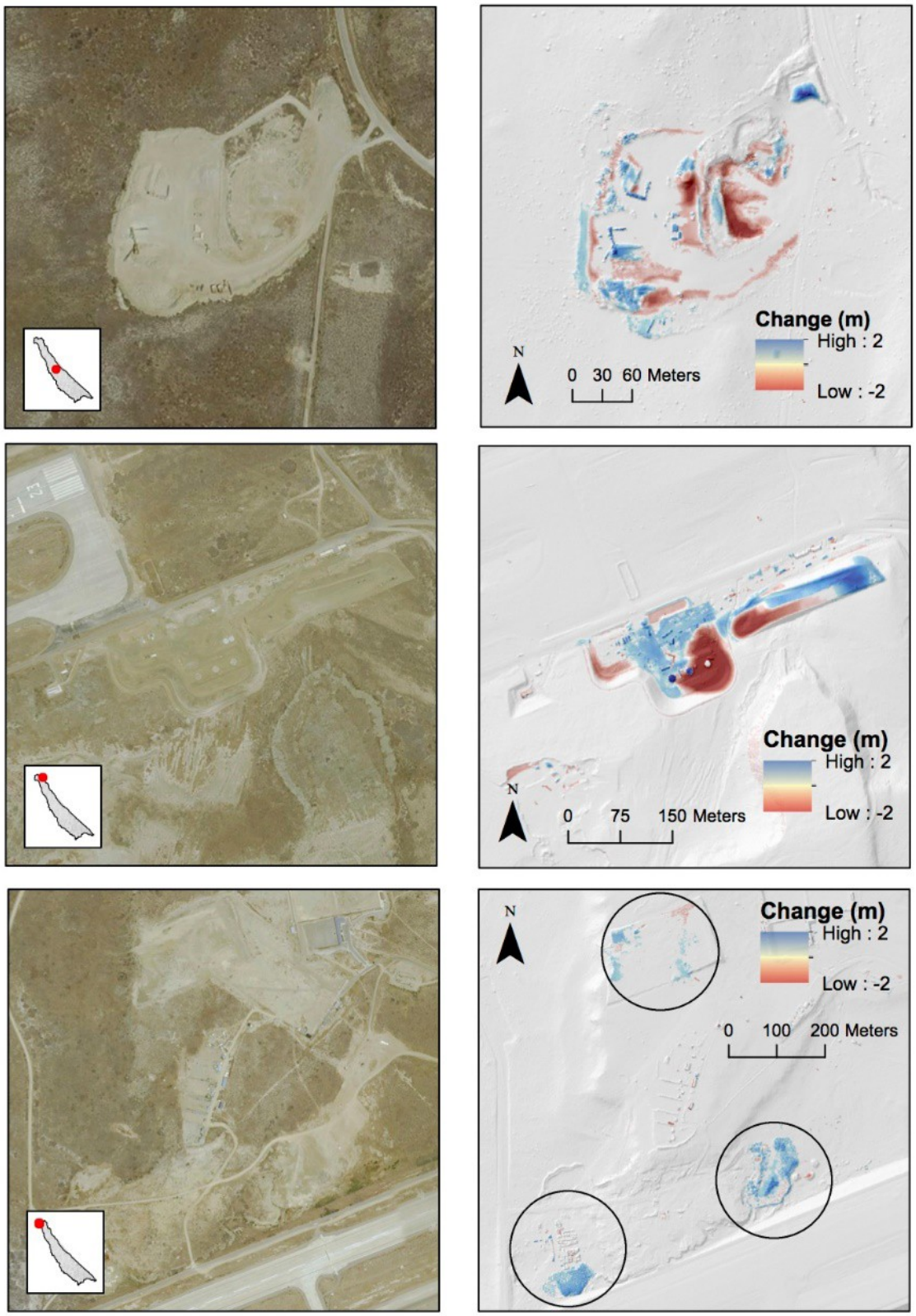

Figure 7. Additional areas of detected vertical change, 2013–2014 (right) and spatially corresponding 2014 aerial photographs (left). Top and bottom images show actively managed quarry sites; middle image shows a construction site.

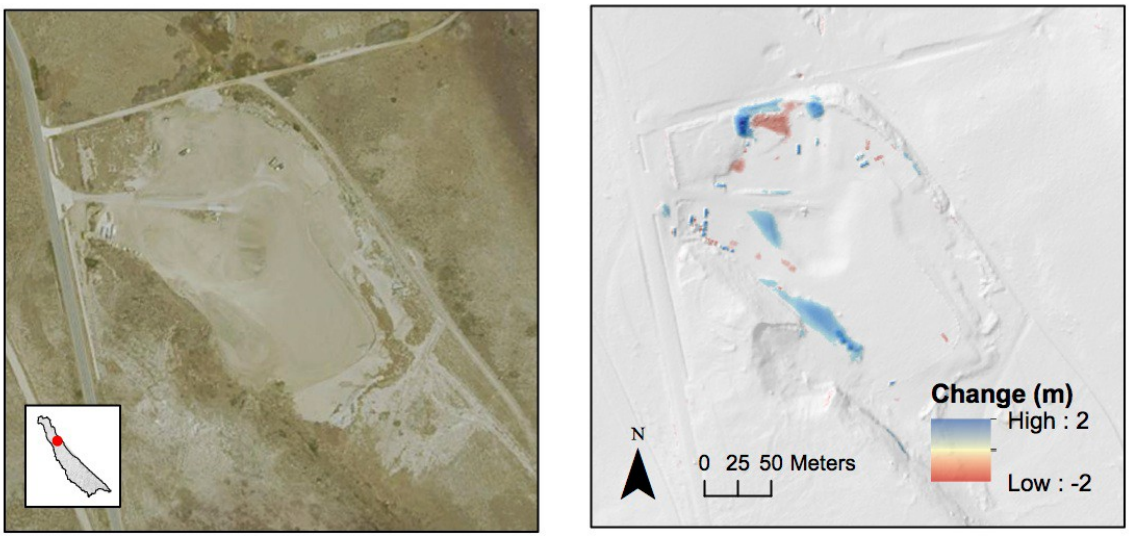

Figure 8. Additional areas of detected vertical change, 2013–2014 (right) and spatially corresponding 2014 aerial photographs (left). This is the site of the San Clemente Island landfill.

The change detection analysis for 2002–2014 and 2013–2014 is significant primarily because it illustrates the capabilities as well as the limitations of the data. Both the 2002 and 2013 DEMs have relatively poor elevation accuracy, which limited the change detection capability. However, analysis of differences between the 2013 and 2014 DEMs still successfully revealed changes with volumes > 2.5 m^3. In this case, the changes are anthropogenic, mostly related to changes to dirt roads, parking lots, construction, and areas of frequent earth moving, such as the island landfill and quarries, rather than due to military training activities.

Future high-quality LiDAR flights that produce data comparable to the current data deliverable would significantly increase change detection capability. For example, Young et al. (2009) used airborne LiDAR data with lower change thresholds to successfully detect changes from down to about 1 m^3. Such higher resolution data, should it be collected in the future, would aid monitoring of both natural changes and military impacts.

3.3 EROSION FEATURES

The 2014 DEM deliverable was also used to analyze erosion on San Clemente Island. Erosion features primarily consist of stream networks and associated gullying, though some anthropogenic munitions craters were found.

3.3.1 Erosion Due to Water

We conducted island-wide watershed analysis on San Clemente. For this analysis, the last return DEM was modified to only include elevations above 5 m (navd88), to remove erroneous drainage patterns along the coast and beach areas. Local depressions in the DEM were filled for the hydraulic analysis, and two small dams were neglected. We detected 146,043 individual drainage basins. Most basins were less than 1000 m^2 in planimetric area and located along the coast (Figure 9).

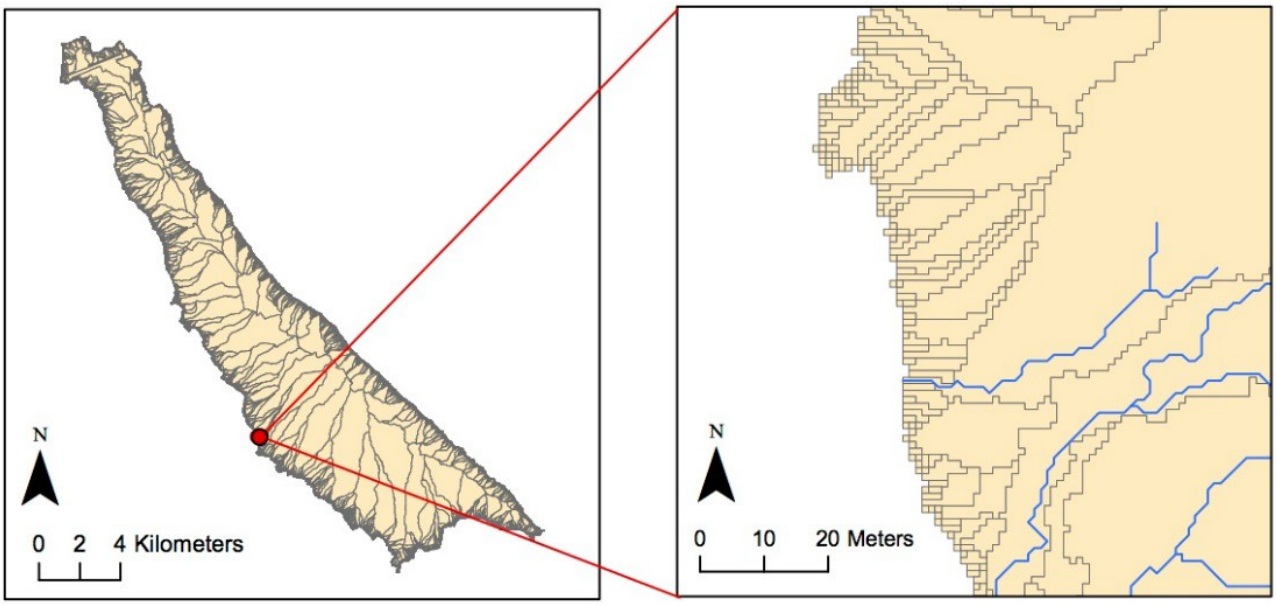

Figure 9. Left: Detected drainage basins on San Clemente. Right: Small basins prevalent along the coast (polygons), and significant drainage pathways (blue lines) in larger basins.

The modified DEM was used for drainage pathway/stream analysis. Flow accumulation analysis (surface area that drains into a raster cell) was conducted and cells with accumulations less than 1000 m^2 were neglected. This resulted in about 2,400 drainage basins used for analysis. A primary ridge extends the length of the island and divides primary drainage southwest and northeast (Figure 10). The largest drainage basins extend from the central island divide to the coast. Sixty one basins drain over 500,000 m^2 each and account for 2/3 of the island's drainage area.

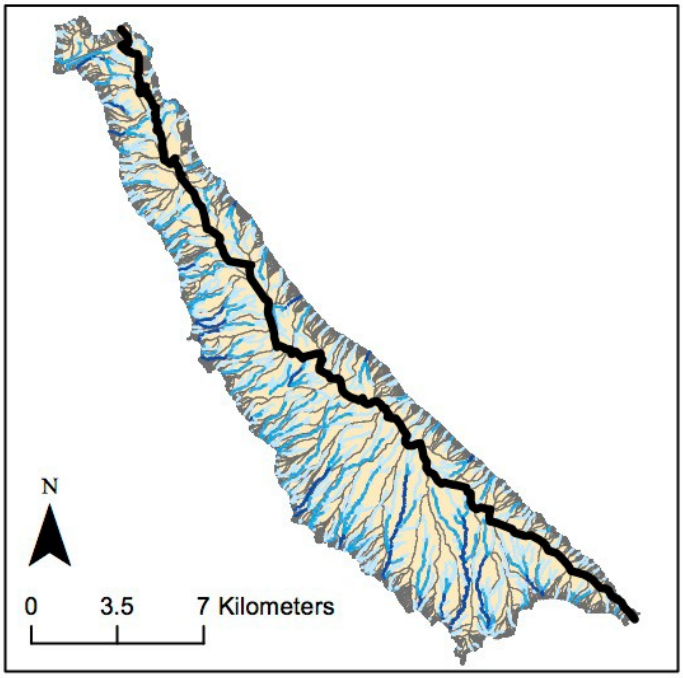

Figure 10. Map showing the central island ridge (thick black line) separating primary drainage directions and stream networks (blue lines).

Most large drainage basins outlets (pour points) are located on the western side of the central ridge, with the largest of these located on the southwest of the island (Figure 11).

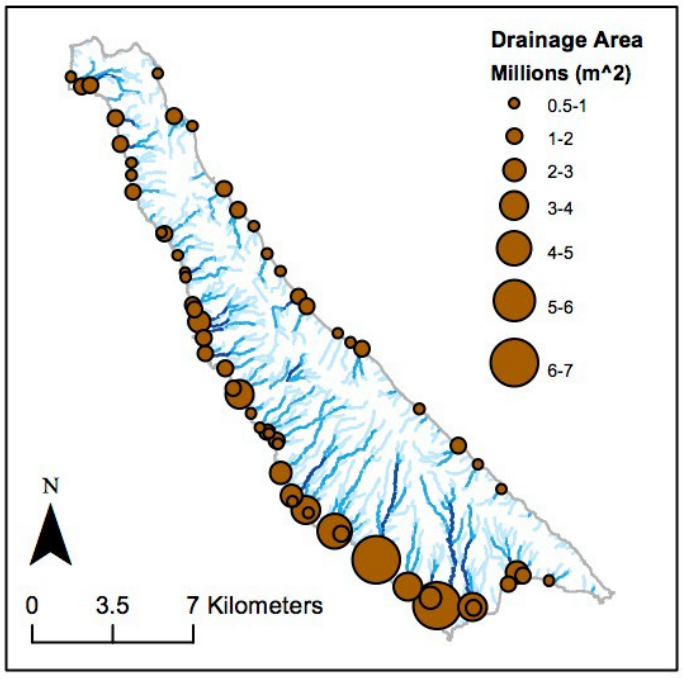

Figure 11. Major pour points (basin drainage outlets) and stream networks. Pour points drainage area values are shown as graduated symbols.

Stream and runoff erosion have developed extensive gully networks on San Clemente Island, particularly on the southwest part of the island (Figure 12). General gully networks were detected programmatically (Figure 13) as clusters of cells with slopes greater than 25°, aggregated to remove holes and join nearby features < 5 m apart. Gully features less than 10 m^2 in area were neglected and holes were filled. This processing represents a preliminary product; additional ground truth and manual editing would be necessary for detailed gully identification.

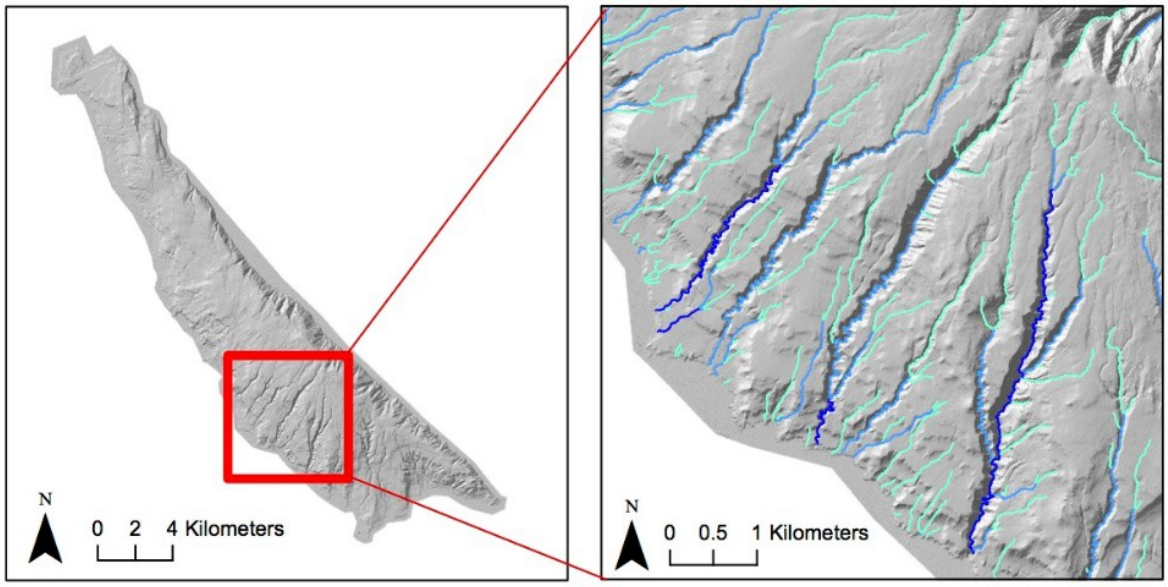

Figure 12. Extensive gully erosion on the southwest part of San Clemente.

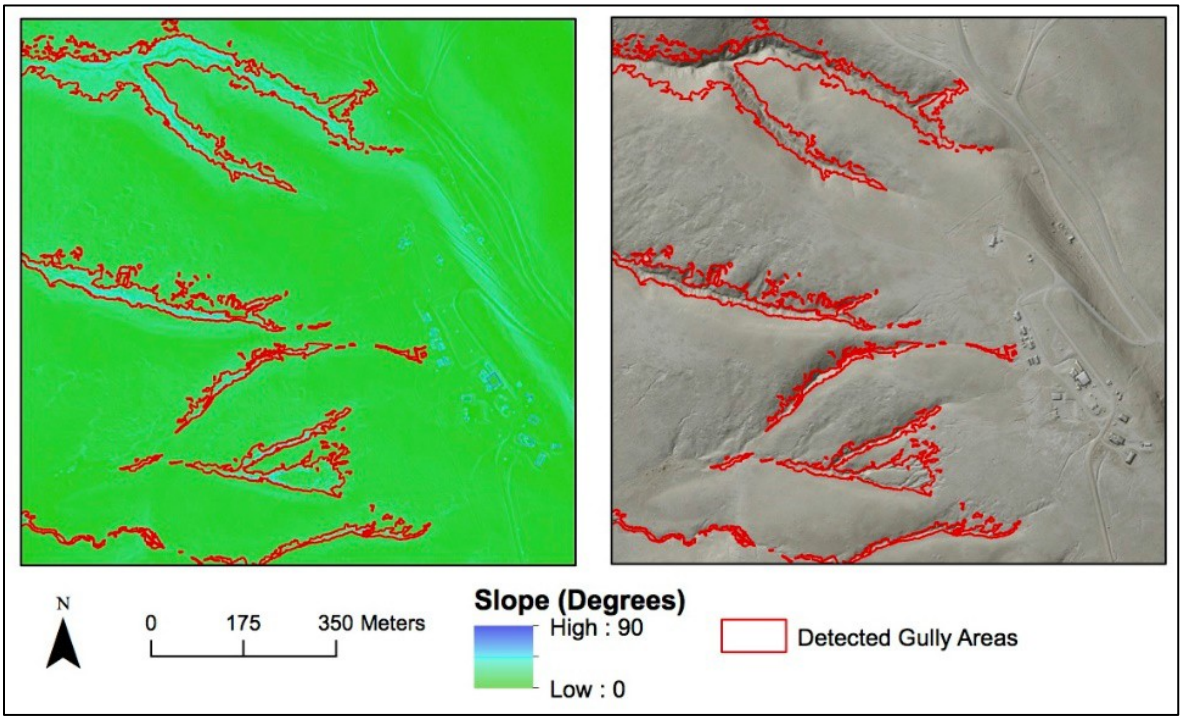

Figure 13. Example of automated gully detection near the central island ridge and training areas.

3.3.2 Erosion Due to Munitions

Anthropogenic erosional features on San Clemente Island include local depressions caused by munitions impacts in target area ranges. Hundreds of detectable craters exist in a range area in on the southwest corner of San Clemente Island (Figure 14). These are typically 3 to 50 m^2 and several meters deep. Bomb craters have likely altered the natural drainage patterns.

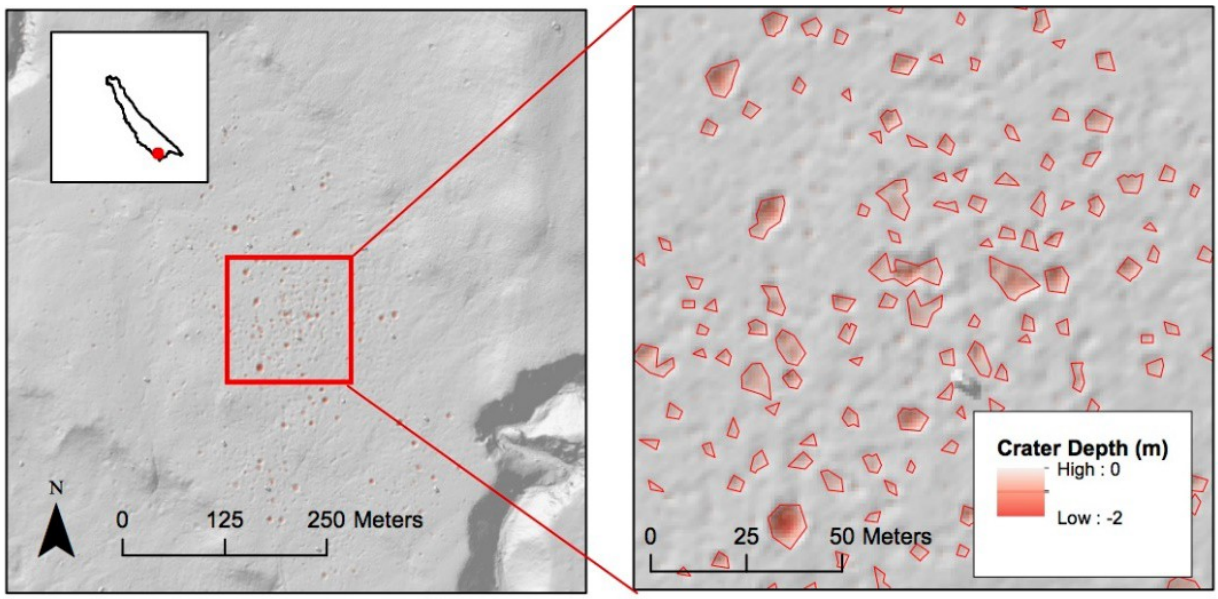

Figure 14. Programmatically detected bomb craters in a target range area on the southwest corner of the island.

4. DATA ANALYSIS: FUTURE POSSIBILITIES

The high-quality data deliverables generated from this work provide extensive possibilities for future data analysis. We briefly explore some of those possibilities in this section. LiDAR-derived rugosity, a measure of topographic variability on small spatial scales, may be a promising method for automatically identifying high-level classes of structures or vegetation (Section 4.1). Preliminary attempts at automated vegetation classification using only the aerial photographs and the ground truth data show that this may also be feasible for some types of vegetation (Section 4.2). Finally, we do not present it here, but the hyperspectral data cubes, with both high spatial and spectral resolution, are powerful data sets that may be leveraged to answer many detailed questions about land cover and change. The addition of temporally coincident ground truth spectra greatly extend the capability of this data set. The limiting factors with the hyperspectral data would be labor hours, processing time, and perhaps computer resources. This very large data set lends itself best to answering specific questions desired by the user, as each question will require its own detailed work flow to be developed.

4.1 CLASSIFICATION USING THE LIDAR DATA: RUGOSITY FILTERS

We tested the feasibility of using rugosity for geomorphic characterization and vegetation identification with promising results. We began by creating the following rugosity rasters from the first return DEM: standard deviation of slope (3 x 3 cell filter window), standard deviation of elevation (3 x 3 cell filter window), range of slope (3 x 3 cell filter window), topographic position index (TPI), 10 x 10 cell filter window; Jenness, 2006), and surface area ratio (Jenness, 2013). Examples of these rugosity metrics are shown in Figure 15.

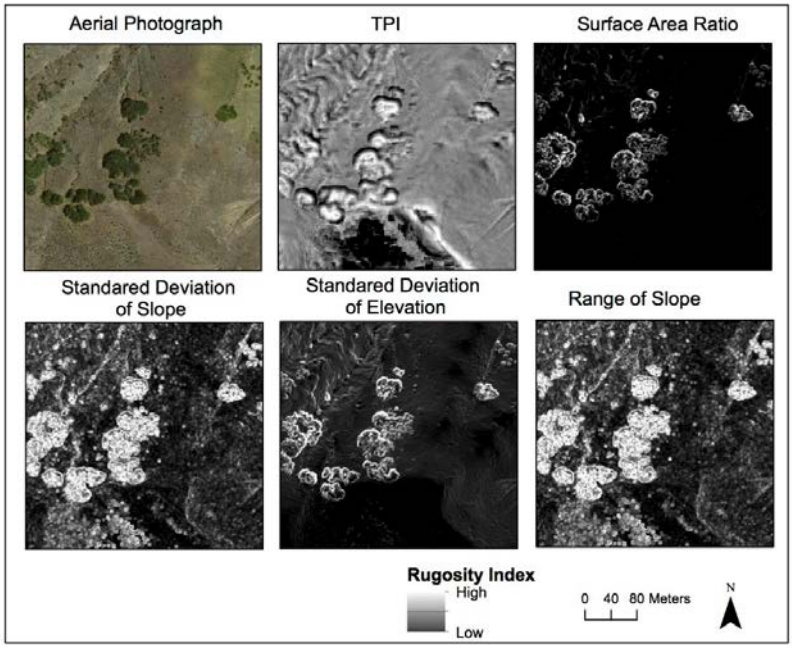

Figure 15. Rugosity metrics for the area shown in the aerial photograph (upper left panel).

We then attempted to use rugosity to identify vegetation and man-made structures. For example, using the standard deviation of slope rugosity filter, a threshold of 10°, and a 100 m^2 minimum area, we could automatically extract polygons of vegetation and man-made structures from the DEM in selected parts of San Clemente Island. These extractions are shown in Figure 16. Each method has its limitations, and this particular method performs poorly on areas with more complex terrain, such as gullies. However, feature detection with rugosity filters appears promising, and may have the potential to be tailored to detect particular targets or vegetation classes, such as low-lying plants versus trees.

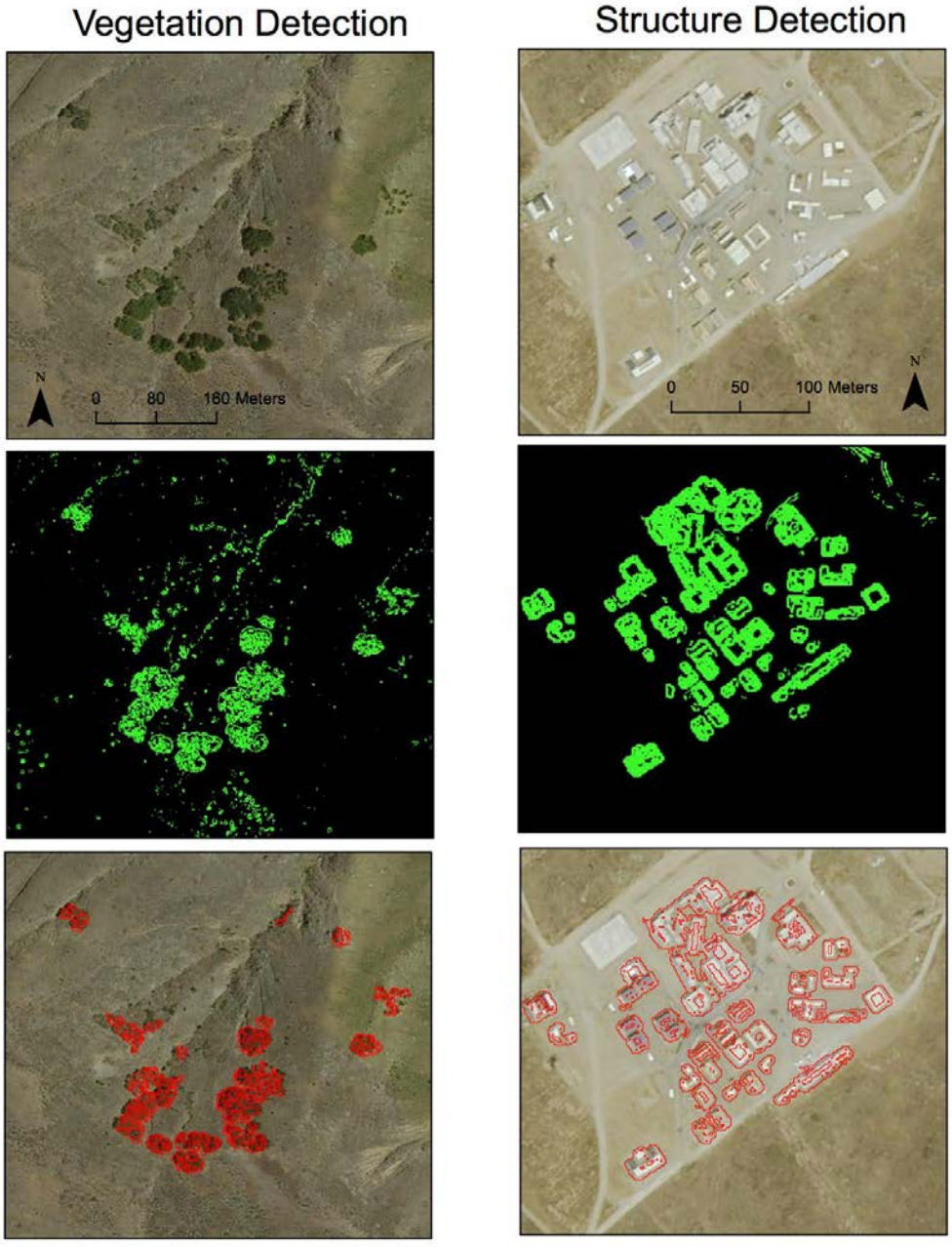

Figure 16. Examples of automated vegetation and structure detection using a rugosity filter on a portion of San Clemente Island.

4.2 VEGETATION CLASSIFICATION USING THE PHOTOGRAPHIC DATA

We also explored the possibility of vegetation and terrain classification using the aerial SLR photographs. Figure 17 (top panel) shows species identified during the ground truth effort in an area on the northwest side of the island.

Using ArcGIS®, we established species signatures in these locations within the photographic data, then applied maximum likelihood classification. The center and bottom panels show the results of the supervised, cell-based maximum likelihood classification of ice plant (identified only to genus) and lemonade berry (*Rhus integrifolia*). Areas of sand were identified via unsupervised isodata cluster terrain classification. This preliminary testing of automated species mapping from the aerial photographs shows promise, though additional field data would be necessary to test the accuracy of the classification algorithms.

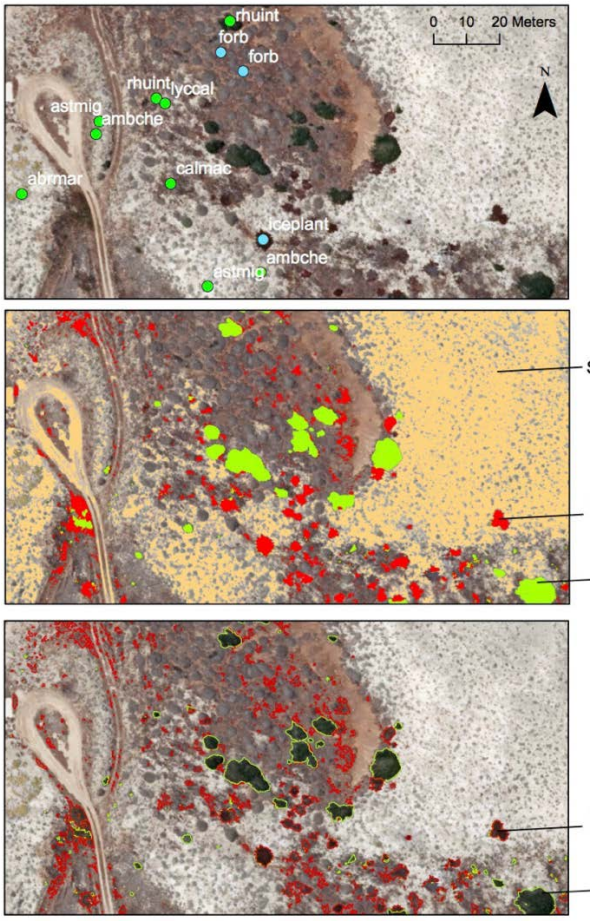

Figure 17. Species identified during the ground truth effort, used to establish species signatures in the photographic data (top). Results of supervised, cell-based maximum likelihood classification of ice plant and sumac (labled "Rhuint") in the same photograph; areas of sand were identified via unsupervised isodata cluster terrain classification (center). Identified spatial outlines of sumac and ice plant, which comprise 3.1 and 4.4% of the area, respectively (bottom).

5. SUMMARY

In summary, this work effort generated several high-resolution remote sensing datasets of San Clemente Island to support PACFLT's natural resources and environmental management needs. In particular, high-resolution LiDAR data were collected to support analysis of erosion related to both military training impacts and natural causes. The data deliverables have been detailed.

Data delivered includes high-resolution LiDAR point data with embedded color information (10-cm vertical accuracy), georeferenced first and last return digital elevation models (1 m x 1 m grid), high-resolution hyperspectral data cubes (126 bands with ~5-nm spectral resolution), and georeferenced aerial photographs. Data collection flights were flown in September and October 2014. Supporting ground truth data collected by SSC Pacific and PACFLT have also been included in the data distribution.

The data deliverables serve as a baseline dataset to be used as a point of comparison for future monitoring. Using existing DEMs from 2002 and 2013 in conjunction with the current DEM deliverable, we evaluated historic topographic change for the time periods 2002–2014 and 2013–2014. Erosion and accretion with volumes >2.5 m^3 were successfully detected. These changes were primarily attributable to changes to dirt roads and parking lots. The relatively poor accuracy of the historical DEMs limited change detection capability for these time periods; nonetheless, they enabled us to show proof of concept for SCI. We estimate that future flights generating LiDAR datasets of comparable quality to the current deliverable will support detection of volume changes on the order of 1 m^3.

Erosion analysis was carried out for the island, using the bare earth DEM deliverable. Most erosion is gullying due to water runoff. Depressions due to training activities is seen in the target range areas on in the southwest corner of SCI. Here munitions impacts have created hundreds of craters, typically several meters deep and 3 to 50 m^2 in area. These craters will likely have altered natural drainage patterns.

Finally, the high resolution data deliverables generated from this work provide extensive possibilities for future data analysis. We briefly explored some of these possibilities. Rugosity metrics derived from the LiDAR data showed promise for automatically identifying structures such as vegetation and buildings, and could possibly be refined to identify subclasses of these structures. Using the aerial photographs in conjunction with the ground truth data, we automated the identification of the shrub *Rhus integrifolia* within the same image as our training dataset. This method could be extended and refined to identify other vegetation throughout the island. Lastly, the hyperspectral data cubes, with both high spatial and spectral resolution, may be leveraged to answer many questions about ground cover. The addition of coincident ground truth spectra further enhances the capability of this powerful dataset.

To best support monitoring and management of the natural resources on San Clemente Island, return flights roughly every two years are suggested.

REFERENCES

Jenness, J. 2006. "Topographic Position Index Extension for ArcView." Jenness Enterprises. Flagstaff, AZ

Jenness, J. 2013. "DEM Surface Tools." Jenness Enterprises. Flagstaff, AZ.

Young, A. P., R. T. Guza, R. E. Flick, W. C. O'Reilly, and R. Gutierrez. 2009. "Rain, Waves, and Short-term Evolution of Composite Seacliffs in Southern California." *Marine Geology 267*:1–7.

.

REPORT DOCUMENTATION PAGE

Form Approved
OMB No. 0704-01-0188

PLEASE DO NOT RETURN YOUR FORM TO THE ABOVE ADDRESS.

1. REPORT DATE *(DD-MM-YYYY)*	**2. REPORT TYPE**	**3. DATES COVERED** *(From - To)*
December 2016	Final	

4. TITLE AND SUBTITLE

San Clemente Island Baseline LiDAR Mapping
Final Report

5a. CONTRACT NUMBER

5b. GRANT NUMBER

5c. PROGRAM ELEMENT NUMBER

6. AUTHORS

D. Bart Chadwick
Jennifer Ayers
William Wild
SSC Pacific

Adam Young
Ken Melville
Luc Lenain
Nick Statom
Reinhard Flick
SIO UCSD

5d. PROJECT NUMBER

5e. TASK NUMBER

5f. WORK UNIT NUMBER

7. PERFORMING ORGANIZATION NAME(S) AND ADDRESS(ES)

SSC Pacific
53560 Hull Street
San Diego, CA 92152–5001

8. PERFORMING ORGANIZATION REPORT NUMBER

TR 3032

9. SPONSORING/MONITORING AGENCY NAME(S) AND ADDRESS(ES)

Commander, U.S. Pacific Fleet
250 Makalapa Drive
Pearl Harbor, HI 96860-3131

10. SPONSOR/MONITOR'S ACRONYM(S)

Commander NSF PACFLT

11. SPONSOR/MONITOR'S REPORT NUMBER(S)

12. DISTRIBUTION/AVAILABILITY STATEMENT

Approved for public release.

13. SUPPLEMENTARY NOTES

14. ABSTRACT

U.S. Pacific Fleet (PACFLT) requires high-resolution topographic data of San Clemente Island (SCI) to support management of the island's natural resources and environment. Such a dataset will enable tracking of changes in erosion patterns, which may be precursors to training impacts on species and their habitats. In response to this need, this work effort generated several high-resolution, georeferenced aerial remote sensing data sets of SCI. This report describes the data deliverables and the analysis that has been done with them.

15. SUBJECT TERMS

LiDAR data analysis; hyperspectral data; digital elevation models; ground truth; historical topographical change detection

16. SECURITY CLASSIFICATION OF:			**17. LIMITATION OF ABSTRACT**	**18. NUMBER OF PAGES**	**19a. NAME OF RESPONSIBLE PERSON**
a. REPORT	**b. ABSTRACT**	**c. THIS PAGE**			Jennifer Ayers
U	U	U	U	35	**19B. TELEPHONE NUMBER** *(Include area code)* (619) 553-9915

INITIAL DISTRIBUTION

84300	Library	(1)
71705	D. B. Chadwick	(1)
71750	J. Ayers	(1)
71760	W. Wild	(1)

Defense Technical Information Center
Fort Belvoir, VA 22060–6218 (1)

Approved for public release.

SSC Pacific
San Diego, CA 92152-5001